Thermoluminescence properties of ZnO and ZnO:Yb nanophosphors

U. Pal, R. Meléndrez, V. Chernov, and M. Barboza-Flores

Citation: Applied Physics Letters **89**, 183118 (2006); doi: 10.1063/1.2374866
View online: http://dx.doi.org/10.1063/1.2374866
View Table of Contents: http://scitation.aip.org/content/aip/journal/apl/89/18?ver=pdfcov
Published by the AIP Publishing

Thermoluminescence properties of ZnO and ZnO:Yb nanophosphors

U. Pal[a)]
Instituto Física, Universidad Autónoma de Puebla, Apartado Postal J-48, Puebla 72570, Mexico

R. Meléndrez, V. Chernov, and M. Barboza-Flores
Centro de Investigación en Física, Universidad de Sonora, Apartado Postal 5-088, Hermosillo, Sonora 83190, Mexico

(Received 6 July 2006; accepted 19 September 2006; published online 3 November 2006)

ZnO and ZnO:Yb thermoluminescence nanophosphors have been developed and tested under beta radiation. Spherical nanoparticles of sizes ranging from 130 to 1200 nm were prepared through a glycol mediated chemical synthesis. The Yb doping had a thermoluminescence quenching effect compared to undoped ZnO. The 5% Yb concentration produced a low fading, a single thermoluminescence glow peak structure, and a dose linearity behavior adequate for thermoluminescence dosimetry applications. The ZnO:Yb nanophosphor has a great potential as a dosimeter for monitoring in ionizing radiation fields. © *2006 American Institute of Physics*.
[DOI: 10.1063/1.2374866]

Recently, investigation on nanostructured ZnO has been greatly stimulated due to its potential applications in optoelectronics, sensors, transducers, and biomedical applications.[1,2] ZnO is a wide band gap semiconductor (3.37 eV at 300 K) usually exhibiting visible luminescence due to the existence of intrinsic or extrinsic defects. The defect related emissions seem to depend on the nanostructure morphologies, defect types, and concentrations resulting in emissions from ultraviolet (UV) to red.[3] Although, the photoluminescence (PL) and the carrier recombination processes in some ZnO nanostructures and the role of the defects involved have been studied,[4] the exact nature of these emissions is still controversial.

Photoluminescence is the luminescence emitted following absorption of light by a material and involves transitions inside the band gap without transport of charges. Thermally stimulated luminescence, commonly called thermoluminescence (TL), takes place when a material (phosphor) is exposed to UV or ionizing radiation, and later thermally stimulated. The radiation exposure of the phosphor materials creates electron-hole pairs which eventually get trapped in localized trap-states existing inside the band gap of the material, and most of the charge carriers remain trapped afterwards. The localized trap states in a material are generated due to the existing intrinsic defects or the defects generated by radiation exposure. The thermal stimulation frees the trapped electrons (holes) which travel through the conduction (valence) band, opposite charges recombine, and light emission is produced through a radiative recombination process. The charge trapping and thermally stimulated recombination mechanisms are important for radiation dose assessment. In a good dosimetric material, the number of trapped charge carriers and in consequence the integrated intensity of the thermally stimulated light emission (recombination) are proportional to the exposure dose. Though there exists several excellent dosimetric phosphors with high TL efficiency and linear dose behavior,[5–7] still there is a great interest in searching for efficient dosimetric materials and their dose assessment to meet technological challenges and our understanding of radiation effects on human and nanoelectronic systems. Such an understanding is indispensable in a number of areas including radiation therapy for cancer treatment and extended human presence in outer space. Some nanostructured materials have been recently investigated in relation to their TL properties including $Y_3Al_5O_{12}$ (YAG),[8] ZnO,[9] ZrO_2,[10] and $CaSO_4$:Dy,[11] which show great potential for dosimetric applications. In the present letter we report on the synthesis, TL properties, and dosimetric behavior of undoped and Yb doped nanostructured ZnO phosphors.

The undoped and doped ZnO nanostructures were prepared through a glycol mediated chemical synthesis. In a typical synthesis process 0.025*M* of anhydrous zinc acetate $[(C_2H_3O_2)_2Zn$, Aldrich, 99.99%] was added to 1*M* of ethyleneglycol (Baker) in a round bottom flux and heated at 440 K temperature for 2 h. After cooling to room temperature (RT), the white mixture was filtered and washed by ethanol and water repeatedly and dried at RT. For Yb doping, $YbCl_3 \cdot 6H_2O$ (Alfa Aesar, 99.9%) of 1, 2, and 5 at. % (nominal) were added to the reaction mixture before heating.

Morphology of the undoped and doped samples was studied using a JEOL JSM LV 5600 scanning electron microscope (SEM) with a Noran SuperDry analytical system attached. Figure 1(a) shows a typical SEM micrograph for the undoped sample. Spherical ZnO particles of sizes ranging from 130 to 1200 nm were formed in the samples. In general, the average size of the particles decreases with the increase of Yb doping concentration, and varied from 392 nm for undoped to 245 nm for 5% Yb doped samples. X-ray

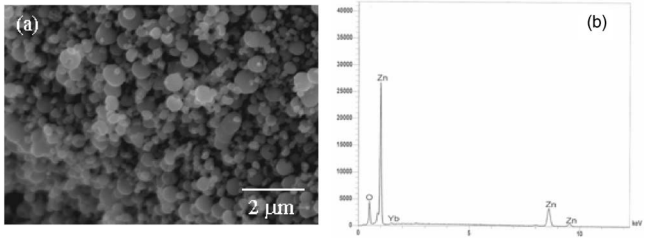

FIG. 1. Typical SEM image for the undoped ZnO (a) and EDS spectrum for the ZnO nanostructures doped with 1% Yb (b).

[a)]Author to whom correspondence should be addressed; FAX: +52-222-2295611; electronic mail: upal@sirio.ifuap.buap.mx

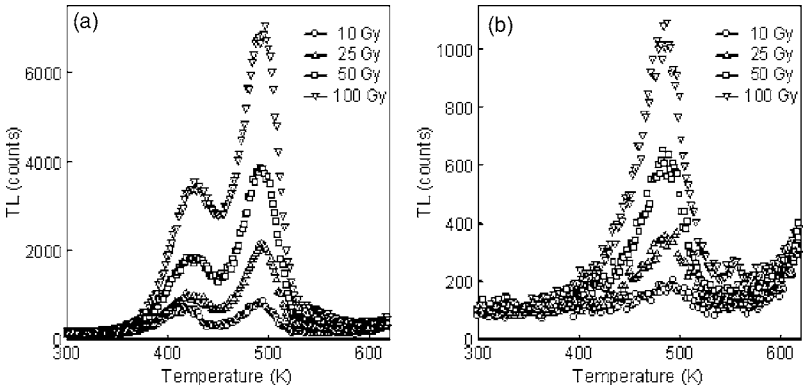

FIG. 2. TL glow curves taken after irradiation at indicated doses: (a) undoped ZnO and (b) 5% Yb doped ZnO.

diffraction studies revealed polycrystalline nature of the ZnO particles (not presented). The composition of the samples was estimated through energy dispersion spectroscopy (EDS) measurements [Fig. 1(b)]. We can see only the emission peaks of O, Zn, and Yb in the samples. The concentration of O in the samples was 55.2 and 55.5 at. % for the undoped and doped samples, respectively. The EDS estimated Yb concentrations for the 1%, 2%, and 5% nominally doped samples were about 0.5%, 0.7%, and 0.8% respectively. The concentration of Zn reduced from 44.8 to 43.7 at. % on Yb doping.

The TL measurements were performed using a Harshaw TLD system 4000 and a Risø TL/OSL System model TL-DA-15. The photomultiplier tube used for measuring TL emission had maximum detection efficiency around 400 nm. Beta irradiation exposures were done using a (^{90}Sr–^{90}Y) source having an activity of 0.04 Ci and 5 Gy/min dose rate. The heating rate of TL readouts was 5 K/s. The recorded TL glow curves were analyzed by a homemade deconvolution program based on the nonlinear least-squares Marquardt method.

Figure 2 shows typical TL glow curves of undoped and 5% Yb doped ZnO, after exposed to beta radiation ranging from 10 to 100 Gy at RT. For the undoped sample, the TL glow curves exhibit two peaks with maxima at 420 and 490 K. The Yb doping induces a TL quenching effect and changes the TL curve shape. The TL glow curves of the 5% Yb doped sample reveal a single peak with maximum at 480 K and intensity of about six times lower then the maximal intensity of the undoped sample. The ZnO samples with 1 and 2 at. % Yb show unstructured less intense TL between 400 and 570 K.

The kinetic processes involved in the TL of the nanostructured ZnO phosphors could be extracted using a deconvolution computer fitting program. A nonlinear least-squares Marquardt fitting method, capable of simultaneously processing up to first or second order kinetic TL glow peaks,[12] was used to calculate the activation energy E (eV), the frequency factors s (s^{-1}), the maximum peak temperature, and the peak area. The TL glow peaks were fitted to first and second order kinetic equations given by Eqs. (1) and (2), respectively,[12]

$$S(T) = S_0 \exp\left[-\frac{sk_BT^2}{\beta E}\exp\left(-\frac{E}{k_BT}\right)\left(1-\frac{2k_BT}{E}\right)\right], \quad (1)$$

$$S(T) = S_0\left[1+\frac{sk_BT^2}{\beta E}\exp\left(-\frac{E}{k_BT}\right)\left(1-\frac{2k_BT}{E}\right)\right]^{-1}, \quad (2)$$

$S(T)$ represents the total light emitted during heating from temperature T up to a full emptying of the TL traps, which is also proportional to the current concentration of filled traps. The TL signal $\Delta S(T)$ is proportional to some amount of light emitted during heating from temperature T to $T+\Delta T$ and can be presented as $\Delta S(T)=S(T)-S(T+\Delta T)$, S_0 is the total TL signal emitted during the heating process (the peak area). β is the heating rate and k_B is Boltzmann's constant.

Figure 3 displays the TL glow curves as well as its fitted components for the undoped ZnO and ZnO:Yb (5%) samples. It is interesting to observe that the undoped ZnO displays first and second order kinetic TL glow peak components at 420 and 490 K, with $E=0.8$ and 1.2 eV and $s=7\times10^8$ and 1×10^{12} s^{-1}, respectively. However, the TL glow curve of ZnO:Yb (5%) shows a single first order peak at 480 K with $E=0.8$ eV and $s=4.4\times10^7$ s^{-1}.

The dose dependences of the peak areas obtained with the deconvolution procedure for undoped and 5% Yb doped ZnO samples are shown in Fig. 4. Certainly, the 5% Yb doping concentration, besides improving the TL performance of the ZnO nanostructures, also improves noticeably its dose

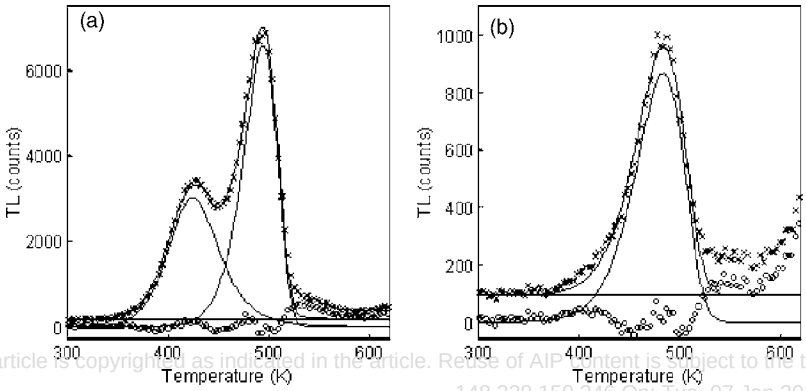

FIG. 3. Computer deconvoluted of TL glow curves for undoped ZnO (a) and ZnO doped with 5% Yb (b) exposed to 100 Gy of beta radiation. ZnO displays two TL glow peak components at 420 K (second order) and 490 K (first order), with activation energies of 0.8 and 1.2 eV. The TL glow curve of ZnO:Yb (5%) shows a first order peak at 480 K with an activation energy of 0.8 eV.

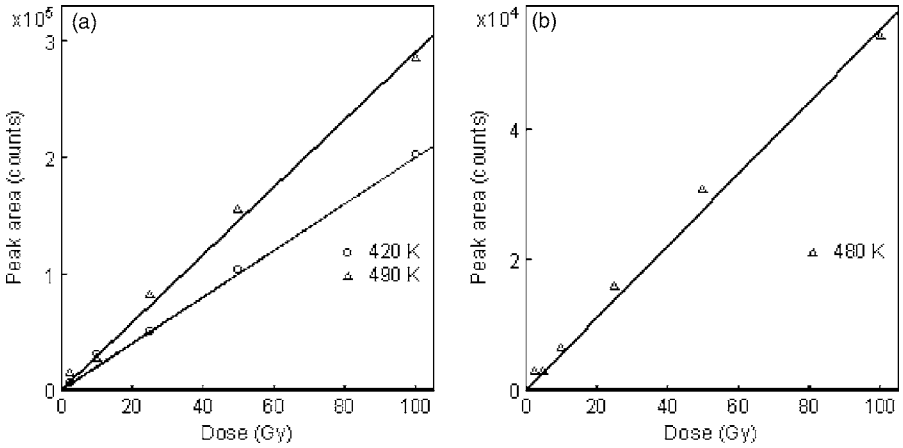

FIG. 4. Dose dependences of the peak areas: (a) undoped ZnO and (b) ZnO doped with 5% Yb.

linearity response. In spite of the TL quenching effect of doping, the advantage resulting from the induced dose linearity is noteworthy. The TL efficiency (light emitted during heating from 320 to 520 K) of ZnO:Yb was about ten times lower than the undoped nanophosphor. We must mention that the low 0–10 Gy dose behavior seen in Yb (5%) doped ZnO sample was also observed for all other dopant concentrations used in the present work. Interestingly, the 5% doped sample revels a clean high temperature glow peak with high TL intensity. The existence of such TL glow peaks is related to the electrons (or holes) trapped at deep localized trap states, which are adequate for dosimetric applications due to characteristic low TL fading losses. Room temperature TL fading losses are related to the charge carriers trapped at shallow trap states localized close to the conduction (electrons) or valence (holes) bands. The RT instabilities produce charge detrapping and eventual recombination of the charge carriers, without contribution of the real dose given to the sample. It was observed that the undoped ZnO sample exhibited a 10% TL fading loss in 600 s time period after irradiation with 100 Gy beta-ray dose. The TL fading observed in ZnO:Yb (5%) phosphor under the same conditions was insignificant.

It is important to mention that the undoped ZnO nanophosphor displays a characteristic RT afterglow (AG) signal after irradiation with 100 Gy beta-ray dose, which decreases as a function of Yb concentration. The highest afterglow comes from the undoped ZnO specimen and is about 3.5, 3.1, and 2.5 times greater than 5%, 2%, and 1% Yb doped ZnO, respectively. The AG decay process refers to the RT light emitted signal after the sample is irradiated; it corresponds to the radiative recombination of the charges trapped at shallow traps (350–550 K), freed by RT instabilities. It is noticeable that the Yb doping decreases the AG up to a background signal for 5% doping concentration. It is evident that the Yb doping improves the RT stability of trapped charges at shallow/low temperature localized trap states. The radiative and nonradiative recombinations related to the AG and TL thermal fadings may hinder the dose assessment provided by the ZnO phosphor material, since these recombinations involve some charge carriers produced by radiation exposure that will not be associated with thermally stable filled trap states. It may result in an underestimation of the irradiation dose given to the dosimeter sample. A good dosimeter material should have low AG and TL fading properties. From the AG and TL data of our ZnO:Yb (5%) sample, it is unambiguous that this phosphor qualify as low AG and TL fading materials suitable for dosimetric applications in ionizing radiation fields.

In summary, we have developed a ZnO:Yb (5%) nanophospor with low AG and TL fadings at RT which exhibits a linear dose behavior for β rays in the 0–100 Gy dose range. The nanophospors have great potential as a dosimeter for monitoring in ionizing radiation fields.

The authors acknowledge UC-MEXUS and CONACyT, Mexico for their financial support through Grant Nos. CN-05-215 and 46269, respectively.

[1]Zhong Lin Wang, J. Phys.: Condens. Matter **16**, R829 (2004).
[2]Ü. Özgür, Ya. I. Alivov, C. Liu, A. Teke, M. A. Reshchikov, S. Doğan, V. Avrutin, S.-J. Cho, and H. Morkoç, J. Appl. Phys. **98**, 041301 (2005).
[3]A. B. Djurisić, Y. H. Leung, K. H. Tam, L. Ding, W. K. Ge, H. Y. Chen, and S. Gwo, Appl. Phys. Lett. **88**, 103107 (2006).
[4]A. F. Vladimir, A. A. Khan, A. B. Alexander, X. Faxian, and L. Jianlin, Phys. Rev. B **73**, 165317 (2006).
[5]S. W. S. McKeever, *Thermoluminescence of Solids* (Cambridge University Press, Cambridge, 1985), Chap. 6, pp. 205–234.
[6]K. Mahesh, P. S. Weng, and C. Furetta, *Thermoluminescence of Solids and Its Applications* (Nuclear Technology, Kent, England, 1989), Chap. 4, pp. 85–94.
[7]S. W. S. McKeever, M. Moscovitch, and P. D. Townsend, *Thermoluminescence Dosimetry Materials: Properties and Uses* (Nuclear Technology, Kent, England, 1995), Chaps. 3–6, pp. 85–94.
[8]R. A. Rodriguez, E. De la Rosa, R. Meléndrez, P. Salas, J. Castañeda, M. V. Felix, and M. Barboza-Flores, Opt. Mater. (Amsterdam, Neth.) **27**, 1240 (2005).
[9]C. Cruz-Vazquez, R. Bernal, S. E. Burruel-Ibarra, and H. Grijalva-Monteverde, Opt. Mater. (Amsterdam, Neth.) **27**, 1235 (2005).
[10]T. Rivera, L. Olvera, J. Azorin, R. Sosa, M. Barrera, A. M. Soto, and C. Furetta, Radiat. Eff. Defects Solids **161**, 91 (2006).
[11]N. Salah, P. D. Sahare, S. P. Lochab, and P. Kumar, Nucl. Tracks Radiat. Meas. **41**, 40 (2006).
[12]R. Chen and S. W. S. McKeever, *Theory of Thermoluminescence and Related Phenomena* (World Scientific, Singapore, 1997), Chap. 2, pp. 29–31.